Parity anomaly and spin transmutation in quantum spin Hall Josephson junctions

Yang Peng,[1] Yuval Vinkler-Aviv,[1] Piet W. Brouwer,[1] Leonid I. Glazman,[2] and Felix von Oppen[1]

[1] *Dahlem Center for Complex Quantum Systems and Fachbereich Physik, Freie Universität Berlin, 14195 Berlin, Germany*
[2] *Department of Physics, Yale University, New Haven, Connecticut 06520, USA*

We study the Josephson effect in a quantum spin Hall system coupled to a localized magnetic impurity. As a consequence of the fermion parity anomaly, the spin of the combined system of impurity and spin-Hall edge alternates between half-integer and integer values when the superconducting phase difference across the junction advances by 2π. This leads to characteristic differences in the splittings of the spin multiplets by exchange coupling and single-ion anisotropy at phase differences, for which time-reserval symmetry is preserved. We discuss the resulting 8π-periodic (or $\mathbb{Z}_4$) fractional Josephson effect in the context of recent experiments.

Introduction.—The fractional Josephson effect [1–3] constitutes one of the most striking effects heralding topological superconductivity [4, 5]. In a Josephson junction made from conventional superconductors, the Josephson current is carried by Cooper pairs and is 2π periodic in the phase difference applied to the junction. When the junction connects topological superconductors [6–9], the coupling of Majorana bound states across the junction allows a Josephson current to flow by coherent transfer of single electrons, resulting in 4π periodicity in the phase difference. Robust 4π periodicity requires that time-reversal symmetry be broken through proximity coupling to a magnetic insulator or an applied magnetic field [6]. A fractional Josephson effect can occur in time-reversal-symmetric junctions as a consequence of electron-electron interactions [10]. In the limit of strong interactions, this 8π-periodic effect can be understood in terms of domain walls carrying $\mathbb{Z}_4$ parafermions, enabling tunneling of $e/2$ quasiparticles between the superconductors.

Recent experiments on superconductor – quantum spin Hall – superconductor junctions show intriguing evidence for 4π-periodic Josephson currents. One experiment probes Shapiro steps and shows that the first Shapiro step is absent [11]. A second experiment reports that the Josephson radiation emitted by a biased junction is also consistent with 4π periodicity [12]. These results are surprising as both experiments were performed without explicitly breaking time-reversal symmetry so that basic theory would predict a dissipative 2π-periodic behavior when neglecting electron-electron interactions, or an 8π-periodic behavior when taking interactions into account.

These expectations are based on considering pristine quantum spin Hall Josephson junctions with a fully gapped bulk and a single helical channel propagating along its edges. Density modulations in actual quantum spin Hall samples are widely believed to induce puddles of electrons in addition to the helical edge channels [13]. When these puddles host an odd number of electrons, charging effects turn them into magnetic impurities which are exchange coupled to the helical edge channels. In this paper, we discuss the fractional Josephson effect in realistic quantum spin Hall Josephson junctions which include such magnetic impurities.

The effects of magnetic impurities on quantum spin Hall edge channels have been intensively studied in the absence of superconductivity [14–17]. In the high-temperature limit, a magnetic impurity induces backscattering between the Kramers pair of helical edge channels and thus deviations from a quantized conductance in a two-terminal measurement. As the temperature is lowered, the impurity spin is increasingly Kondo screened by the helical edge channel and perfect conductance quantization is recovered in the zero-temperature limit. In the presence of superconductivity, the Kondo effect is quenched by the superconducting gap so that one may expect that magnetic impurities field more prominent consequences. Here, we assume that the Kondo temperature is well below the superconducting gap so that we can safely neglect the effects of Kondo screening.

We find that coupling to magnetic impurities alters the behavior of quantum spin Hall Josephson junctions qualitatively. The Josephson current generically becomes 8π periodic, replacing the dissipative 2π-periodic effect in the absence of this coupling. This can be viewed as a variant of the $\mathbb{Z}_4$ Josephson effect. Indeed, unlike its classical counterpart, coupling to a quantum spin preserves time-reversal symmetry and interactions are effectively included through the local-moment formation, which is quite reminiscent of the ingredients of the $\mathbb{Z}_4$ fractional Josephson effect. Thus, our results show that this remarkable effect is considerably more generic than one might have previously thought.

Moreover, the present setting emphasizes a remarkable mechanism for producing an 8π-periodic fractional Josephson effect. As a result of the fermion parity anomaly [3], the spin of the helical edge effectively changes by $\hbar/2$ when the superconducting phase difference is advanced by 2π. This adiabatically transmutes the combined spin of helical edge and magnetic impurity between half-integer and integer values, with their characteristically different behavior in the presence of time-reversal symmetry as described by the Kramers theorem.

Quantum spin Hall Josephson junctions.—We begin

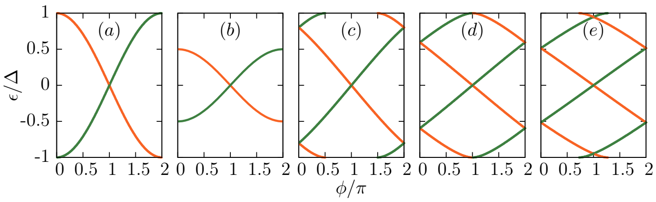

Figure 1. Andreev spectrum of quantum spin Hall Josephson junctions with different length of the junction. (a) $\Delta L/v = 0$; (b) $\Delta L/v = 0$ in the presence of backscattering due to a Zeeman field; (c) $\Delta L/v = 0.8$; (d) $\Delta L/v = \pi/2$; (e) $\Delta L/v = 2$. The green curves correspond to Andreev states consisting of a superposition of an up-spin electron and an Andreev-reflected hole. The orange curves are for the particle-hole conjugated states.

by reviewing the Andreev spectrum of quantum spin Hall Josephson junctions in the absence of magnetic impurities [3]. Consider a quantum spin Hall edge with counterpropagating edge modes, placed in between two superconductors whose phases differ by ϕ. The subgap spectrum of such a Josephson junction as a function of ϕ is shown in Fig. 1.

In the short junction limit $L \to 0$, the subgap spectrum contains a single particle-hole symmetric pair of Andreev states [see Fig. 1(a)]. Both Andreev levels emanate from and merge into the quasiparticle continuum. Hence, when the phase advances proportional to an applied bias voltage V, the junction exhibits an *ac* Josephson effect with the conventional frequency $\dot{\phi} = 2eV/\hbar$ and energy dissipation rate $(2\Delta)(\dot{\phi}/2\pi)$.

The dissipative nature of the Josephson effect is closely related to the helical nature of the edge modes and the ensuing absence of backscattering. When introducing backscattering into the junction by breaking time-reversal symmetry through an applied magnetic field or proximity coupling to a magnetic insulator, the Andreev levels no longer merge with the quasiparticle continuum [see Fig. 1(b)], quenching dissipation in the small-voltage limit [6]. Moreover, the *ac* Josephson effect occurs at half the conventional frequency, i.e., at $eV/\hbar$, as fermion number parity is conserved. Indeed, the level crossing at $\phi = \pi$ is protected by fermion number parity so that the individual Andreev levels are 4π periodic in the phase difference ϕ. This can be viewed as a consequence of the fermion parity anomaly: As a result of the quantum spin Hall effect, the fermion parity of the edge changes when the superconducting phase difference is advanced by 2π, requiring a phase change of 4π for a full period.

Additional subgap levels appear for longer junctions, see Figs. 1(c) and (d). The structure of level crossings in these spectra is not only controlled by fermion parity, but also by time-reversal symmetry. While time reversal is generally broken by the phase difference across the junction (resulting in a nonzero Josephson current flowing in the junction), it remains unbroken at phase differences equal to integer multiples of π.

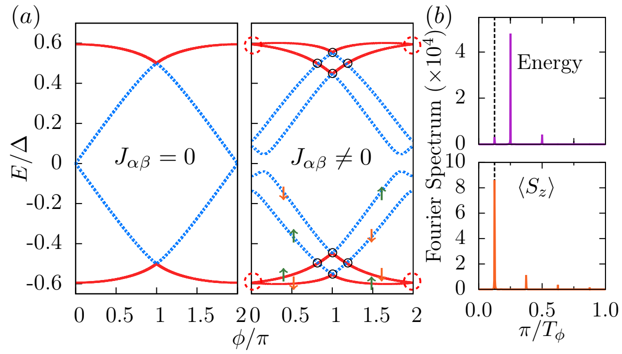

Figure 2. (a) Generic many-body spectrum for the quantum spin Hall Josephson junction ($\Delta L/v = \pi/2$) without impurity spin (left) and with coupling to the impurity spin (right, J_α/L is of order $0.1 \sim 1$). The red solid and blue dashed curves indicate even and odd fermion parity, respectively, with the discontinuity in parity at $\phi = \pi$ originating from the merging of Andreev levels with the continuum, see Fig. 1(d). The crossings at and near $\phi = \pi$ indicated by black circles are between states of opposite fermion parity. The crossings between states with even fermion parity at $\phi = 0$ and 2π, highlighted by red dashed circles, are protected by time reversal. The arrows indicate the impurity-spin polarization along the z-axis. (b) Fourier transforms of the many-body ground state energy or, equivalently, the Josephson current (upper panel) and of the expectation value of the impurity spin polarization $\langle S_z \rangle$ (lower panel) as a function of the phase difference ϕ. The 8π-periodic harmonics are indicated by the vertical dashed lines.

Coupling to magnetic impurity.—We now consider the coupling of the edge channel to a magnetic impurity with spin S. Generically, disorder in conjunction with the strong spin-orbit coupling will remove any symmetry other than time reversal which we assume to be broken only by the applied superconducting phase difference. Thus, we focus on the general Hamiltonian

$$H_S = \sum_{\alpha,\beta} J_{\alpha\beta} \hat{S}^\alpha \hat{\sigma}^\beta(0) + \sum_\alpha D_\alpha (\hat{S}^\alpha)^2 \tag{1}$$

for the impurity spin $\hat{\mathbf{S}}$. The first term describes the exchange coupling between the impurity spin and the helical edge, with $\hat{\sigma}^\alpha(0) = \sum_{i,j} \psi_i^\dagger(0)(\sigma^\alpha)_{ij}\psi_j(0)$ denoting the local spin density of the helical edge at the position $x = 0$ of the coupling to the impurity. The operator $\psi_i(x)$ annihilates an electron with spin projection i at position x, and σ^α denotes the $\alpha = x, y, z$ Pauli matrix. The second term describes a general single-ion anisotropy of the impurity spin with strengths D_α. Time reversal implies that the exchange couplings are real, but otherwise arbitrary.

Josephson effect.—Analyzing the Josephson effect of the quantum spin Hall edge channel coupled to the magnetic impurity is greatly simplified by the discrete nature of the subgap spectrum. For definiteness, consider an intermediate-length junction whose subgap spectrum has exactly two positive-energy subgap states $\epsilon_n(\phi)$ $(n = 1, 2)$ at all values of the phase difference as in Fig. 1(d). (This convenient choice is used in our numerical illustrations but not essential for our results.) Then, we can analyze the low-energy (many-body) spectrum of the junction coupled to the impurity spin in the finite-dimensional basis of low-energy states spanned by the product of occupation states of the two subgap Bogoliubov quasiparticles (yielding four basis states) and the $2S+1$ spin states of the spin-S impurity. The low-energy many-body spectrum is effectively decoupled from the quasiparticle continuum as long as the exchange couplings $J_{\alpha\beta}$ are not too large. The corresponding Hamiltonian is readily derived by retaining only the contributions of the two positive-energy subgap Bogoliubov operators γ_n to the edge-state electron operators (see [18] for details). In this limit, the total Hamiltonian can be approximated as $H = H_e + H_S$ with

$$H_e = \sum_n \epsilon_n(\phi)\left(\gamma_n^\dagger\gamma_n - \frac{1}{2}\right) \quad (2)$$

the Hamiltonian of the bare edge.

Consider coupling the quantum spin Hall edge states to a spin-1/2 impurity. Figure 2(a) shows the many-body spectrum of H_e in Eq. (2), i.e., of the bare edge (left panel), and of $H = H_e + H_S$ for a generic choice of exchange couplings $J_{\alpha\beta}$ (right panel). The spectrum of the coupled edge is best understood by analyzing the nature of the degeneracies at phase differences equal to integer multiples of π. The degeneracies at and near $\phi = \pi$ are protected by fermion parity. Here, level crossings occur between states with even and odd occupations of the Bogoliubov quasiparticles of the edge. In contrast, the level crossings at $\phi = 0$ and $\phi = 2\pi$ occur between states of the same fermion parity and are Kramers degeneracies reflecting time-reversal symmetry.

In the present system, a Kramers degeneracy appears when the Bogoliubov quasiparticles γ_n of the edge are either both empty or both occupied, leading to a half-integer spin of the combined system of edge and impurity. Specifically, the lower (higher) energy crossing in Fig. 2(a) corresponds to states in which the quasiparticle states are both empty (occupied). Away from $\phi = 0$ and 2π, time reversal is broken and the Kramers degeneracies are lifted. This interpretation is corroborated by further restricting the Hamiltonian H for small ϕ to the low-energy subspace of empty quasiparticle states. In this limit, the spin density $\hat{\sigma}^\alpha(0)$ of the edge only has a nonzero z component $\hat{\sigma}^z(0) = -\epsilon\phi/[2v(1+\kappa L)^2]$ and the Hamiltonian simplifies to

$$H \simeq -\sum_\alpha B^\alpha S^\alpha + \text{const} \quad (3)$$

with the effective Zeeman field $\mathbf{B} = [\epsilon\phi/2v(1 + \kappa L)^2]\sum_\alpha J_{\alpha z}\hat{\mathbf{e}}_\alpha$. Here, we use the subgap energy $\epsilon = \Delta\cos(\epsilon L/v)$ and $\kappa = \sqrt{\Delta^2 - \epsilon^2}/v$.

The four nondegenerate states at intermediate energies for $\phi = 0$ [see Fig. 2(a)] have overall single occupation of the quasiparticle states, leading to a combined edge-impurity system with integer spin. Unlike in the odd-integer spin case, time reversal does not enforce a degeneracy of the many-body spectrum in this case. Writing the Hamiltonian for small ϕ in this subspace using the basis $|\uparrow\rangle = \gamma_1^\dagger|\text{gs}\rangle$ and $|\downarrow\rangle = \gamma_2^\dagger|\text{gs}\rangle$ (with $\gamma_1|\text{gs}\rangle = \gamma_2|\text{gs}\rangle = 0$) for the states of the edge (with corresponding Pauli matrices ρ_α), we find the effective Hamiltonian

$$H \simeq \frac{\kappa}{2(1+\kappa L)}\left[\sum_\alpha J_{\alpha+}S^\alpha\rho_+ + \text{h.c.}\right] \quad (4)$$

Generically, this Hamiltonian has no degeneracies.

With this understanding, the many-body spectrum in Fig. 2(a) reveals a remarkable fact: The total spin of the edge-impurity system alternates between half-integer and integer spin when the superconducting phase difference advances adiabatically from $\phi = 0$ to $\phi = 2\pi$. This spin transmutation is a direct consequence of the parity anomaly. As the phase difference changes by 2π, the fermion parity of the edge changes by virtue of the quantum spin Hall effect. Consequently, also the spin of the edge changes by $\hbar/2$. This change in spin has important consequences for the periodicity of the Josephson effect. Indeed, adiabatically following the energy levels in Fig. 2(a), we find that they are 8π periodic, corresponding to an *ac* Josephson frequency of $eV/2\hbar$. Due to the spin transmutation, the system passes through successive Kramers degeneracies only after advancing the superconducting phase difference by 4π, requiring a phase change of 8π for completing a full period. Note also that starting with the ground state at $\phi = 0$, the many-body state remains well below the quasiparticle continuum for all ϕ, so that the *ac* Josephson effect remains nondissipative at a sufficiently small bias.

The polarization of the impurity spin varies with the superconducting phase difference in an 8π-periodic manner. When adiabatically varying the superconducting phase difference, the spin orientation remains unchanged at the Kramers crossings and flips in the vicinity of the avoided crossings where the edge-impurity system is in an integer-spin state. This variation of the spin with ϕ is illustrated in Fig. 2(a).

These results for $S = 1/2$ impurities are in fact generic and persist for higher-spin impurities. As an illlustration, consider the results for an $S = 1$ impurity in Fig. 3. First consider panel (d) which shows results for generic values of $J_{\alpha\beta}$ and D_α. Unlike in the $S = 1/2$ case, the low-energy states are now integer spin states and thus nondegenerate, while the intermediate-energy states have half-integer spin and are Kramers degenerate at $\phi = 0$

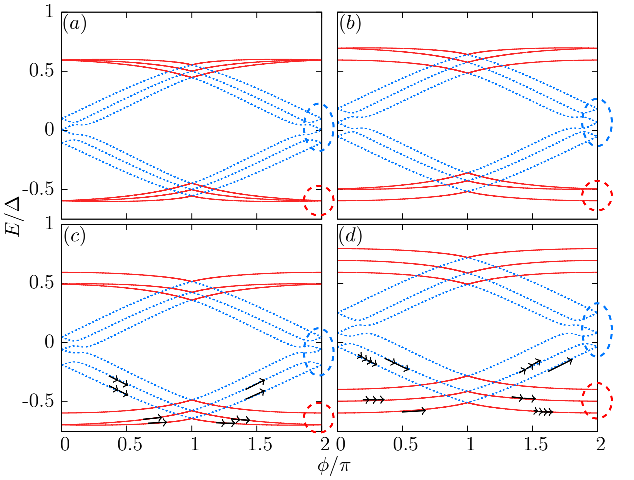

Figure 3. Many-body spectrum for a quantum spin Hall edge coupled to an $S = 1$ impurity. The red solid and blue dashed curves correspond to many-body states with even and odd fermion parity, respectively. Spectra correspond to (a) vanishing single-ion anisotropy, (b) easy-plane anisotropy $D_z > 0$, (c) easy-axis anisotropy $D_z < 0$, and (d) generic single-ion anisotropy with $D_x, D_y, D_z \neq 0$. The degeneracies at $\phi = 2\pi$ (as well as their partners at $\phi = 0$) highlighted by blue dashed circles are Kramers degeneracies. Degeneracies highlighted by red circles are lifted by introducing generic single-ion anisotropy. Subsequent 2π periods for an adiabatic evolution of ϕ are indicated by increasing numbers of arrows.

and 2π. Nevertheless, the 8π periodicity remains intact.

Different periodicities can occur for nongeneric choices of the couplings $J_{\alpha\beta}$ and D_α. In the absence of any single-ion anisotropy [see Fig. 3(a)], the many-body spectrum does not decouple from the quasiparticle continuum and the Josephson effect becomes dissipative and 2π periodic. The same result is obtained for easy-plane anisotropy, with one of the single-ion anisotropies being positive and the others equal to zero, see Fig. 3(b). Finally, easy-axis anisotropy makes the junction nondissipative and 4π periodic as shown in Fig. 3(c).

Discussion.—We find that generically, coupling to a magnetic impurity makes the Josephson effect in quantum spin Hall systems 8π periodic. The 8π periodicity relies only on time-reversal symmetry, the parity anomaly, and the absence of fine tuning such as the absence of interactions or the presence of spin conservation.

This general conclusion requires two comments. First, while the Josephson current is 8π periodic, with a frequency $eV/2\hbar$ of the *ac* Josephson effect, this may actually not be the dominant Fourier component observable in experiment. Indeed, it is evident from Fig. 2 that the 8π-periodic cycle consists of two rather similar 4π sections. The magnitude of the splitting of the two sections is controlled by the strength of the exchange coupling. As long as this exchange splitting remains weak compared to the superconducting gap, the dominant Fourier component of the Josephson current is 4π periodic. This is shown in Fig. 2(b), together with the Fourier analysis of the expectation value of the impurity spin which has a dominant 8π-periodic harmonic. It is interesting to note that this result for the Josephson current is different from the realization of the $\mathbb{Z}_4$ Josephson effect discussed by Zhang and Kane [10] which has a dominant 8π-periodic Fourier component.

Second, it is important to realize that so far, our results consider only the electronic system and neglect coupling to other degrees of freedom such as phonons or the electromagnetic environment. Relaxing this restriction introduces inelastic relaxation processes which may be crucial for determining the experimentally observed periodicity. While relaxation between states of opposite fermion parity may be quite slow, relaxation beween states of the same fermion parity should be considerably more efficient. Observation of the 8π periodicity requires that the latter relaxation processes are slow compared to the period in which the 8π cycle is traversed. Indeed, the two 4π sections of the 8π cycle involve states of the same fermion parity, so that one would always remain in the lower-energy state if the cycle is traversed slowly on the time scale of parity-conserving relaxation processes. This would make the observed Josephson effect 4π rather than 8π periodic.

It is intriguing to compare these results to the recent experiments on quantum spin Hall junctions which observe Shapiro steps and Josephson radiation consistent with 4π periodicity [11, 12]. Our results provide an interesting scenario that is in principle consistent with these observations. At the same time, this is by no means the only explanation of a 4π-periodic Josephson effect in this system. An alternative scenario considers relaxation processes in a pristine quantum spin Hall junction. Consider an intermediate-length junction with at least two positive-energy Andreev states for any phase difference. When both of these Andreev states are occupied, the two quasiparticles can relax inelastically by recombining into a Cooper pair. Two positive-energy quasiparticles are created every time the phase difference advances by 4π. Thus, if their recombination into a Cooper pair is an efficient process, one would also observe a 4π-periodic Josephson effect. It is an interesting problem for future research to devise experimental probes which distinguish between these alternative scenarios for a 4π-periodic Josephson effect in quantum spin Hall Josephson junctions.

Acknowledgments.—We acknowledge financial support by the Deutsche Forschungsgemeinschaft (CRC 183 as well as Priority Program 1666), the Minerva Foundation, the Alexander-von-Humboldt Foundation, and NSF Grant DMR-1603243. Part of this work was performed at the Aspen Center for Physics, which is supported by National Science Foundation grant PHY-1066293.

[1] A. Y. Kitaev, Phys.-Usp. **44**, 131 (2001).
[2] H.-J. Kwon, K. Sengupta, and V. M. Yakovenko, Euro. Phys. J. B **37**, 349 (2004).
[3] L. Fu and C. L. Kane, Phys. Rev. B **79**, 161408 (2009).
[4] J. Alicea, Rep. Prog. Phys. **75** (2012), 10.1088/0034-4885/75/7/076501.
[5] C. W. J. Beenakker, Annu. Rev. Con. Mat. Phys. **4**, 113 (2013).
[6] L. Fu and C. L. Kane, Phys. Rev. Lett. **100**, 096407 (2008).
[7] R. M. Lutchyn, J. D. Sau, and S. Das Sarma, Phys. Rev. Lett. **105**, 077001 (2010).
[8] Y. Oreg, G. Refael, and F. von Oppen, Phys. Rev. Lett. **105**, 177002 (2010).
[9] J. Alicea, Y. Oreg, G. Refael, F. von Oppen, and M. P. A. Fisher, Nat. Phys. **7**, 412 (2011).
[10] F. Zhang and C. L. Kane, Phys. Rev. Lett. **113**, 036401 (2014).
[11] E. Bocquillon, R. S. Deacon, J. Wiedenmann, P. Leubner, T. M. Klapwijk, C. Brüne, K. Ishibashi, H. Buhmann, and L. W. Molenkamp, arXiv preprint arXiv:1601.08055 (2016).
[12] R. S. Deacon, J. Wiedenmann, E. Bocquillon, T. M. Klapwijk, P. Leubner, C. Brüne, S. Tarucha, K. Ishibashi, H. Buhmann, and L. W. Molenkamp, arXiv preprint arXiv:1603.09611 (2016).
[13] J. I. Väyrynen, M. Goldstein, and L. I. Glazman, Phys. Rev. Lett. **110**, 216402 (2013).
[14] J. Maciejko, C. Liu, Y. Oreg, X.-L. Qi, C. Wu, and S.-C. Zhang, Phys. Rev. Lett. **102**, 256803 (2009).
[15] Y. Tanaka, A. Furusaki, and K. A. Matveev, Phys. Rev. Lett. **106**, 236402 (2011).
[16] V. Cheianov and L. I. Glazman, Phys. Rev. Lett. **110**, 206803 (2013).
[17] B. L. Altshuler, I. L. Aleiner, and V. I. Yudson, Phys. Rev. Lett. **111**, 086401 (2013).
[18] Supplemental material available online.
[19] Y. Peng, F. Pientka, E. Berg, Y. Oreg, and F. von Oppen, Phys. Rev. B **94**, 085409 (2016).

SUPPLEMENTAL MATERIAL

ANDREEV BOUND STATES

The Hamiltonian for the quantum spin Hall Josephson junction takes the form $H = \frac{1}{2}\Psi^\dagger\mathcal{H}\Psi$ with Nambu spinor $\Psi = (\psi_\uparrow, \psi_\downarrow, \psi_\downarrow^\dagger, -\psi_\uparrow^\dagger)^T$ in terms of electron operators and the Bogoliubov-de Gennes Hamiltonian

$$\mathcal{H} = vp\sigma_z\tau_z + \Delta(x)\tau_x, \tag{1}$$

where x (p) denotes the coordinate (momentum) along the quantum spin Hall insulator edge, v is the edge-mode velocity, and σ_j and τ_j are Pauli matrices in spin and Nambu (particle-hole) space, respectively. The proximity-induced superconducting gap

$$\begin{aligned}\Delta(x) =& \Delta\left[\theta(-x-L/2) + e^{i\phi\tau_z}\theta(x-L/2)\right] \\ &= \Delta\theta(|x| - \frac{L}{2})e^{i\varphi(x)\tau_z}\end{aligned} \tag{2}$$

has strength $\Delta > 0$ and a phase difference ϕ across the junction region of length L. We have introduced a spatially dependent phase

$$\varphi(x) = \frac{\phi}{L}(x + \frac{L}{2})\theta(\frac{L}{2} - |x|) + \theta(x - \frac{L}{2})\phi. \tag{3}$$

for convenience.

We introduce a local gauge transformation $U = e^{i\varphi(x)\tau_z/2}$ to eliminate the spatial dependence of the superconducting phase, and obtain the transformed Hamiltonian

$$U^\dagger\mathcal{H}U = -iv\partial_x\sigma_z\tau_z + \frac{v\varphi'(x)\sigma_z}{2} + \Delta\theta(|x| - \frac{L}{2})\tau_x, \tag{4}$$

where the prime denotes a derivative with respect to x. We will denote $U^\dagger\mathcal{H}U$ as $\mathcal{H}$ in the following.

To solve for the Andreev bound states, we follow the approach detailed in Ref. [19] to rearrange the Bogoliubov-de Gennes equation $\mathcal{H}\psi = \epsilon\psi$ as

$$i\frac{\partial\psi}{\partial x} = -\frac{1}{v}\sigma_z\tau_z\left[\epsilon - \Delta\theta(|x| - \frac{L}{2})\tau_x - \frac{v\varphi'(x)}{2}\sigma_z\right]\psi. \tag{5}$$

The solution can be written as $\psi(x) = U(x, x_0)\psi(x_0)$ in terms of the state at some reference point x_0. In particular, we have

$$U(\frac{L}{2}, -\frac{L}{2}) = \exp\left\{\frac{i}{v}\sigma_z\tau_z \int_{-\frac{L}{2}}^{\frac{L}{2}} dx' \left[\epsilon - \frac{v\varphi'(x')}{2}\sigma_z\right] = \exp\left(\frac{iEL}{v}\sigma_z\tau_z - \frac{\phi}{2}\tau_z\right)\right\} \tag{6}$$

which connects the states $\psi(L/2) = U(L/2, -L/2)\psi(-L/2)$. We match the properly decaying solutions of the Bogoliubov de-Gennes equation on the left and right of the junction, and obtain the bound state wave functions in the two spin sectors:

$$\Psi_\uparrow(x) = \begin{pmatrix} a_\uparrow A_\uparrow \\ 0 \\ A_\uparrow \\ 0 \end{pmatrix} e^{\kappa_\uparrow(x+\frac{L}{2})}\theta(-x-\frac{L}{2}) + \begin{pmatrix} a_\uparrow A_\uparrow e^{-i(\frac{\phi}{2}-\frac{\epsilon}{v}L)} \\ 0 \\ A_\uparrow e^{i(\frac{\phi}{2}-\frac{\epsilon}{v}L)} \\ 0 \end{pmatrix} e^{-\kappa_\uparrow(x-\frac{L}{2})}\theta(x-\frac{L}{2}) + \begin{pmatrix} a_\uparrow A_\uparrow e^{-i(\frac{\phi}{2L}-\frac{\epsilon}{v})(x+\frac{L}{2})} \\ 0 \\ A_\uparrow e^{i(\frac{\phi}{2L}-\frac{\epsilon}{v})(x+\frac{L}{2})} \\ 0 \end{pmatrix} \theta(\frac{L}{2}-|x|) \tag{7}$$

and

$$\Psi_\downarrow(x) = \begin{pmatrix} 0 \\ A_\downarrow \\ 0 \\ a_\downarrow A_\downarrow \end{pmatrix} e^{\kappa_\downarrow(x+\frac{L}{2})}\theta(-x-\frac{L}{2}) + \begin{pmatrix} 0 \\ A_\downarrow e^{-i(\frac{\phi}{2}+\frac{\epsilon}{v}L)} \\ 0 \\ a_\downarrow A_\downarrow e^{i(\frac{\phi}{2}+\frac{\epsilon}{v}L)} \end{pmatrix} e^{-\kappa_\downarrow(x-\frac{L}{2})}\theta(x-\frac{L}{2}) + \begin{pmatrix} 0 \\ A_\downarrow e^{-i(\frac{\phi}{2L}+\frac{\epsilon}{v})(x+\frac{L}{2})} \\ 0 \\ a_\downarrow A_\downarrow e^{i(\frac{\phi}{2L}+\frac{\epsilon}{v})(x+\frac{L}{2})} \end{pmatrix} \theta(\frac{L}{2}-|x|) \tag{8}$$

where

$$a_\sigma = \frac{\epsilon}{\Delta} - i\frac{\sqrt{\Delta^2-\epsilon_\sigma^2}}{\Delta}, \qquad |A_\sigma|^2 = \frac{\kappa_\sigma}{2(1+L\kappa_\sigma)}, \qquad \kappa_\sigma = \frac{\sqrt{\Delta^2-\epsilon_\sigma^2}}{v} \tag{9}$$

with $\sigma =\uparrow,\downarrow$, and ϵ_σ is the positive eigenvalue in each spin sector given by the relation

$$\epsilon_\uparrow/\Delta = \begin{cases} \cos(\frac{\phi}{2} - \frac{\epsilon_\uparrow}{v}L) & \sin(\frac{\phi}{2} - \frac{\epsilon_\uparrow}{v}L) < 0 \\ -\cos(\frac{\phi}{2} - \frac{\epsilon_\uparrow}{v}L) & \sin(\frac{\phi}{2} - \frac{\epsilon_\uparrow}{v}L) > 0 \end{cases} \tag{10}$$

and

$$\epsilon_\downarrow/\Delta = \begin{cases} \cos(\frac{\phi}{2} + \frac{\epsilon_\downarrow}{v}L) & \sin(\frac{\phi}{2} + \frac{\epsilon_\downarrow}{v}L) > 0 \\ -\cos(\frac{\phi}{2} + \frac{\epsilon_\downarrow}{v}L) & \sin(\frac{\phi}{2} + \frac{\epsilon_\downarrow}{v}L) < 0 \end{cases}. \tag{11}$$

For ϕ around $2n\pi, n \in \mathbb{Z}$, solutions in both spin sectors can exist simultaneously for $L > 0$. We will consider the situation when at most one solution in each spin sector exists, and write the subgap effective Hamiltonian as

$$H_e = \sum_\sigma \epsilon_\sigma(\phi)(\gamma_\sigma^\dagger\gamma_\sigma - \frac{1}{2}), \tag{12}$$

where γ_σ is the Bogoliubov quasiparticle annihilation operator for the Andreev bound state with spin σ. When projected onto the subspace spanned by the subgap Andreev bound states, the electron annihilation operators for both spins can be written approximately as

$$\begin{aligned} \psi_\uparrow &= a_\uparrow A_\uparrow e^{-ik_\uparrow L/2}\gamma_\uparrow - a_\downarrow^* A_\downarrow^* e^{-ik_\downarrow L/2}\gamma_\downarrow^\dagger \\ \psi_\downarrow &= A_\downarrow e^{-ik_\downarrow L/2}\gamma_\downarrow + A_\uparrow^* e^{-ik_\uparrow L/2}\gamma_\uparrow^\dagger \\ k_{\uparrow,\downarrow} &= \frac{\varphi}{2L} \mp \frac{\epsilon_\sigma}{v}. \end{aligned} \tag{13}$$

COUPLING OF AN EDGE CHANNEL TO A MAGNETIC IMURITY

Consider the Hamiltonian describing the coupling of the edge channel to a magnetic impurity with spin S

$$H_S = \sum_{\alpha,\beta} J_{\alpha\beta}\hat{S}^\alpha\hat{\sigma}^\beta(0) + \sum_\alpha D_\alpha(\hat{S}^\alpha)^2, \tag{14}$$

in which the spin density of the helical edge can be written in term of the Bogoliubov operators

$$\hat{\sigma}^{+} = \psi_{\uparrow}^{\dagger}\psi_{\downarrow} = \left(a_{\uparrow}^{*}e^{i\Delta kL/2} + a_{\downarrow}e^{-i\Delta kL/2}\right) A_{\uparrow}^{*}A_{\downarrow}\gamma_{\uparrow}^{\dagger}\gamma_{\downarrow}$$
$$\hat{\sigma}^{-} = \psi_{\downarrow}^{\dagger}\psi_{\uparrow} = \left(a_{\uparrow}e^{-i\Delta kL/2} + a_{\downarrow}^{*}e^{i\Delta kL/2}\right) A_{\uparrow}A_{\downarrow}^{*}\gamma_{\downarrow}^{\dagger}\gamma_{\uparrow}$$
$$\hat{\sigma}^{x} = \left(\hat{\sigma}^{+} + \hat{\sigma}^{-}\right)/2, \quad \hat{\sigma}^{y} = \left(\hat{\sigma}^{+} + \hat{\sigma}^{-}\right)/2i$$
$$\hat{\sigma}^{z} = \psi_{\uparrow}^{\dagger}\psi_{\uparrow} - \psi_{\downarrow}^{\dagger}\psi_{\downarrow} = \left(|A_{\uparrow}|^{2}(2\gamma_{\uparrow}^{\dagger}\gamma_{\uparrow} - 1) - |A_{\downarrow}|^{2}(2\gamma_{\downarrow}^{\dagger}\gamma_{\downarrow} - 1)\right) + (a_{\uparrow}^{*}a_{\downarrow}^{*}e^{i\Delta kL/2} - e^{-i\Delta kL/2})A_{\uparrow}^{*}A_{\downarrow}^{*}\gamma_{\downarrow}^{\dagger}\gamma_{\uparrow}^{\dagger}$$
$$+(a_{\uparrow}a_{\downarrow}e^{-i\Delta kL/2} - e^{i\Delta kL/2})A_{\uparrow}A_{\downarrow}\gamma_{\uparrow}\gamma_{\downarrow}, \tag{15}$$

where

$$\Delta k = k_{\uparrow} - k_{\downarrow} = -\frac{\epsilon_{\uparrow} + \epsilon_{\downarrow}}{v}. \tag{16}$$

Note that we can also write

$$a_{\uparrow} = \mathrm{Sgn}\sin(\frac{\epsilon_{\uparrow}L}{v} - \frac{\phi}{2})e^{-i\frac{\epsilon_{\uparrow}L}{v}}e^{i\phi/2}, \quad a_{\downarrow} = \mathrm{Sgn}\sin(\frac{\epsilon_{\downarrow}L}{v} + \frac{\phi}{2})e^{-i\frac{\epsilon_{\downarrow}L}{v}}e^{-i\phi/2}, \tag{17}$$

then we have

$$\hat{\sigma}^{+} = \left(\mathrm{Sgn}\sin(\frac{\epsilon_{\uparrow}L}{v} - \frac{\phi}{2}) + \mathrm{Sgn}\sin(\frac{\epsilon_{\downarrow}L}{v} + \frac{\phi}{2})\right) e^{i\frac{(\epsilon_{\uparrow}-\epsilon_{\downarrow})L}{2v}}e^{-i\phi/2}A_{\uparrow}^{*}A_{\downarrow}\gamma_{\uparrow}^{\dagger}\gamma_{\downarrow} \tag{18}$$
$$\hat{\sigma}^{-} = \left(\mathrm{Sgn}\sin(\frac{\epsilon_{\uparrow}L}{v} - \frac{\phi}{2}) + \mathrm{Sgn}\sin(\frac{\epsilon_{\downarrow}L}{v} + \frac{\phi}{2})\right) e^{-i\frac{(\epsilon_{\uparrow}-\epsilon_{\downarrow})L}{2v}}e^{i\phi/2}A_{\uparrow}A_{\downarrow}^{*}\gamma_{\downarrow}^{\dagger}\gamma_{\uparrow} \tag{19}$$

$$\hat{\sigma}^{z} = \left(|A_{\uparrow}|^{2}(2\gamma_{\uparrow}^{\dagger}\gamma_{\uparrow} - 1) - |A_{\downarrow}|^{2}(2\gamma_{\downarrow}^{\dagger}\gamma_{\downarrow} - 1)\right)$$
$$+\left[\mathrm{Sgn}\sin(\frac{\epsilon_{\uparrow}L}{v} - \frac{\phi}{2})\,\mathrm{Sgn}\sin(\frac{\epsilon_{\downarrow}L}{v} + \frac{\phi}{2}) - 1\right]\left(e^{i\frac{(\epsilon_{\uparrow}+\epsilon_{\downarrow})L}{2v}}A_{\uparrow}^{*}A_{\downarrow}^{*}\gamma_{\downarrow}^{\dagger}\gamma_{\uparrow}^{\dagger} + e^{-i\frac{(\epsilon_{\uparrow}+\epsilon_{\downarrow})L}{2v}}A_{\uparrow}A_{\downarrow}\gamma_{\downarrow}^{\dagger}\gamma_{\uparrow}^{\dagger}\right). \tag{20}$$

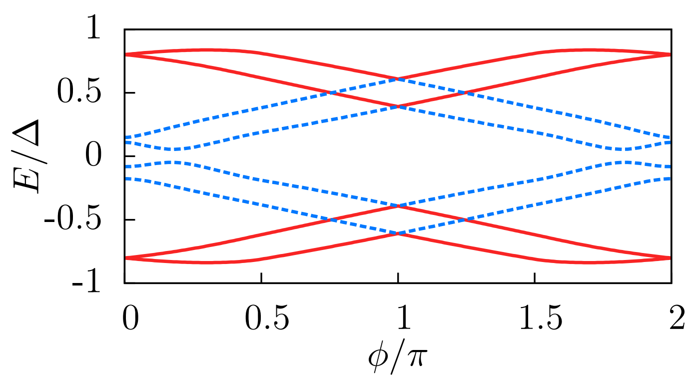

Figure 4. Generic many body spectrum for the quantum spin Hall Josephson junction coupled to a spin-1/2 impurity with $\Delta L/v = 0.8$. The red solid and blue dashed curves indicate that the corresponding many-body states have even and odd fermion parity, respectively.

ANALYSIS AROUND $\phi = 0$

In the case $\Delta L/v \in [0, \pi/2]$, and for ϕ close to 0 we have

$$\mathrm{Sgn}\sin(\frac{\epsilon_{\downarrow}L}{v} - \frac{\phi}{2}) = \mathrm{Sgn}\sin(\frac{\epsilon_{\uparrow}L}{v} + \frac{\phi}{2}) = 1. \tag{21}$$

Let us first focus on the case when $\phi = 0$, we have

$$\epsilon_\uparrow = \epsilon_\downarrow = \Delta \cos\left(\frac{\epsilon_{\uparrow,\downarrow} L}{v}\right). \tag{22}$$

Let us denote the common solution as ϵ.

Now we consider $\phi \ll 1$ and denote $\delta\epsilon = \epsilon_\uparrow - \epsilon_\downarrow$. By Eq. (10) and (11) and condition (21), we have

$$\begin{aligned}\delta\epsilon &= \Delta\left[\cos(\frac{\epsilon_\uparrow}{v}L - \frac{\phi}{2}) - \cos(\frac{\epsilon_\downarrow L}{v} + \frac{\phi}{2})\right] \\ &= \Delta\cos\frac{\phi}{2}\left(\cos\frac{\epsilon_\uparrow L}{v} - \cos\frac{\epsilon_\downarrow L}{v}\right) + \Delta\sin\frac{\phi}{2}\left(\sin\frac{\epsilon_\uparrow L}{v} + \sin\frac{\epsilon_\downarrow L}{v}\right) \\ &\simeq \Delta\sin(\frac{\epsilon L}{v})\phi = \kappa v\phi,\end{aligned} \tag{23}$$

where

$$\kappa = \frac{\sqrt{\Delta^2 - \epsilon^2}}{v}. \tag{24}$$

This is valid up to first order in ϕ.

In this situation, the operators $\hat{\sigma}^+$, $\hat{\sigma}^-$ and $\hat{\sigma}^z$ get simplified as

$$\hat{\sigma}^+ = 2\exp\left[i\left(\kappa L - 1\right)\frac{\phi}{2}\right] A_\uparrow^* A_\downarrow \gamma_\uparrow^\dagger \gamma_\downarrow \tag{25}$$

$$\hat{\sigma}^- = 2\exp\left[-i\left(\kappa L - 1\right)\frac{\phi}{2}\right] A_\uparrow A_\downarrow^* \gamma_\uparrow^\dagger \gamma_\downarrow \tag{26}$$

$$\hat{\sigma}^z = \left|A_\uparrow\right|^2 (2\gamma_\uparrow^\dagger\gamma_\uparrow - 1) - \left|A_\downarrow\right|^2 (2\gamma_\downarrow^\dagger\gamma_\downarrow - 1). \tag{27}$$

Because of this, the total occupation number $N = \gamma_\uparrow^\dagger\gamma_\uparrow + \gamma_\downarrow^\dagger\gamma_\downarrow$ becomes a good quantum number, namely $[N, H] = 0$ where $H = H_e + H_S$. The many body Hilbert space is spanned by the states $|N\alpha\rangle = |N\rangle \otimes |\alpha\rangle$ with $N = 0, 1, 2$ labeling the occupation number of the Andreev bound state and $\alpha = +, -$ labeling the eigenstates of S_z of the impurity spin.

The subspace for $N = 0$ is spanned by $|0+\rangle$, and $|0-\rangle$. The Hamiltonian H in this subspace is represented by a 2 by 2 matrix

$$H^{N=0} = -\epsilon - \frac{\left|A_\uparrow\right|^2 - \left|A_\downarrow\right|^2}{2}\left(J_{zz}\tau_z + J_{+z}\tau_+ + J_{+z}^*\tau_-\right) \tag{28}$$

where $\tau_\pm = (\tau_x \pm i\tau_y)/2$ with $\tau_{x,y,z}$ are Pauli matrices in this two dimensional subspaces.

By using Eq. (9), we have

$$\left|A_\uparrow\right|^2 - \left|A_\downarrow^2\right| \simeq -\frac{\epsilon}{2v(1 + L\kappa)^2}\phi. \tag{29}$$

The subspace with $N = 1$ is spanned by $|\uparrow +\rangle$, $|\downarrow +\rangle$, $|\uparrow -\rangle$, $|\downarrow -\rangle$. The Hamiltonian in this case can be written as

$$H^{N=1} = 2\exp\left[i\left(\kappa L - 1\right)\frac{\phi}{2}\right] A_\uparrow^* A_\downarrow (J_{z+}\tau_z + J_{++}\tau_+ + J_{-+}\tau_-)\rho_+ + h.c. \tag{30}$$

where $\rho_\pm = (\rho_x \pm i\rho_y)/2$ and $\rho_{x,y,z}$ are Pauli matrices in $|\uparrow\rangle, |\downarrow\rangle$ space, and we have neglected terms linear in $\phi \simeq 0$.

An unitary transformation $U = e^{-i\eta\rho_z/2}$ for some $\eta \in [0, \pi/2]$ can always be chosen such that

$$UH^{N=1}U^\dagger = \frac{\kappa}{2(1 + \kappa L)}\left[(J_{z+}\tau_z + J_{++}\tau_+ + J_{-+}\tau_-)\rho_z + h.c.\right] \tag{31}$$

which has the same spectrum as $H^{N=1}$. The four eigenvalues are generically nondegenerate.